

Heavy quark free energies for three quark systems at finite temperature

Kay Hübner and Frithjof Karsch

Physics Department, Brookhaven National Laboratory, Upton, NY 11973, USA

Olaf Kaczmarek and Oliver Vogt

Fakultät für Physik, Universität Bielefeld, D-33615 Bielefeld, Germany

(Dated: February 9, 2022)

We study the free energy of static three quark systems in singlet, octet, decuplet and average color channels in the quenched approximation and in 2-flavor QCD at finite temperature. We show that in the high temperature phase singlet and decuplet free energies of three quark systems are well described by the sum of the free energies of three diquark systems plus self energy contributions of the three quarks. In the confining low temperature phase we find evidence for a Y-shaped flux tube in SU(3) pure gauge theory, which is less evident in 2-flavor QCD due to the onset of string breaking. We also compare the short distance behavior of octet and decuplet free energies to the free energies of single static quarks in the corresponding color representations.

PACS numbers:

I. INTRODUCTION

The study of baryonic systems composed of three static quarks sheds light on the internal structure of the baryon. Lattice calculations have been carried out addressing this question for quite some time now [1, 2, 3, 4, 5, 6, 7, 8]. Of particular interest is the question whether a genuine three body force exists between the quarks below the critical temperature and how the system behaves at finite temperature. At zero temperature the Y-string shape of the color flux tube in baryonic systems is supported by recent calculations in lattice QCD [4, 6, 8]. At finite temperature work so far has concentrated on simulations using maximal abelian gauge [6, 7], showing the existence of a Y-shaped string as well. The Y-Ansatz is also supported by results obtained with the field correlator method [9].

Recently, there have been speculations that hadronic bound states, e. g. also colored QQQ -states, may still exist in the high temperature deconfined phase of QCD and that they could be responsible for the observed strong interactions in the QGP near T_c [10]. This makes it interesting to analyze the force in three quark systems also in non-singlet color configurations that might exist in an overall color neutral thermal medium.

In this paper, we examine the question of the flux tube shape of the QQQ -singlet state below the critical temperature in the quenched approximation of QCD and discuss the appearance of string breaking in 2-flavor QCD. Moreover, above T_c we explore the relation between the free energies in different color channels of the baryonic system and the free energies of QQ -subsystems, and analyze the screening of octet and decuplet free energies at small distances.

This paper is organised as follows: In section II we present the basic observables we use for calculations in different color channels of the heavy three quark system in terms of correlation functions of thermal Wilson lines. In section III we discuss the perturbative behavior of free energies of three quark systems at short distances. In sec-

tion IV we present the details of our simulation, including calculation techniques, gauge fixing and renormalisation procedures. In section V we discuss the behavior of QQQ -free energies obtained in SU(3) pure gauge theory on $32^3 \times 4, 8$ lattices and compare results above T_c with free energies of QQ -systems. Furthermore, we examine the string shape below T_c . Section VI is devoted to a discussion of our results in 2-flavor QCD. In section VII we analyze the screening of octet and decuplet free energies at small distances. Finally, in section VIII, we conclude.

II. STATIC THREE QUARK SYSTEMS IN DIFFERENT COLOR REPRESENTATIONS

In the following we will construct observables for the free energies of static three quark systems in different color channels and introduce the corresponding relation to the expectation values of correlation functions of thermal Wilson lines. Since we are interested in QCD, we restrict ourselves to examine the SU(3) gauge group.

The state of a three quark system as the product of irreducible representations of three quarks in color space can be decomposed into symmetry states

$$3 \otimes 3 \otimes 3 = 1 \oplus 8 \oplus 8' \oplus 10. \quad (1)$$

The singlet is totally anti-symmetric, the first octet anti-symmetric in the first and second, the second octet in the second and third component and the decuplet is totally symmetric.

We now construct observables for static three quark systems represented by suitable combinations of Wilson lines. The derivation is similar to that for two quark systems [11, 12], but more elaborate. We start by defining the thermal Wilson line

$$L(\mathbf{x}) = \prod_{x_4=0}^{N_\tau-1} U_4(\mathbf{x}, x_4). \quad (2)$$

The Polyakov loop is then obtained by $l(\mathbf{x}) = \text{Tr } L(\mathbf{x})$, where the trace is normalised such that $\text{Tr } \mathbf{1} = 3$. For the three quark correlation function of thermal Wilson lines¹ L_1, L_2, L_3 , we have

$$L_1 L_2 L_3 = \sum_s C_{QQQ}^s(\mathbf{x}_1, \mathbf{x}_2, \mathbf{x}_3) P_s, \quad (3)$$

where $s \in \{1, 8, 8', 10\}$ stands for the symmetry states, P_s for the projectors on these states and C_{QQQ}^s for the three point correlator of the thermal Wilson line belonging to that symmetry state. Here we have suppressed the dependence on the temperature T .

Denoting the components of the thermal Wilson lines $L_1^{il}, L_2^{jm}, L_3^{kn}$, where $i, j, k, l, m, n = 1, 2, 3$, we find the projectors P_s by using the Fierz-identity

$$P_1 = \frac{1}{6} \sum_{\sigma(l,m,n)} \epsilon^{lmn} \delta^{il} \delta^{jm} \delta^{kn} \quad (4)$$

$$P_8 = \frac{1}{3} \sum_{\sigma(l,m,n)} \epsilon^{lm} \delta^{il} \delta^{jm} \delta^{kn} \quad (5)$$

$$P_{8'} = \frac{1}{3} \sum_{\sigma(l,m,n)} \epsilon^{nm} \delta^{il} \delta^{jm} \delta^{kn} \quad (6)$$

$$P_{10} = \frac{1}{6} \sum_{\sigma(l,m,n)} \delta^{il} \delta^{jm} \delta^{kn}, \quad (7)$$

where the sums are over all permutations σ of the indices. The P_s satisfy the usual relations for projectors

$$P_s^2 = P_s, \quad \sum_s P_s = \mathbf{1} \quad \text{und} \quad P_s P_t = 0 \quad (8)$$

for $s \neq t$ and $s, t \in \{1, 8, 8', 10\}$. The desired three quark correlators in the different color channels are now obtained by applying

$$C_{QQQ}^s = \frac{\text{Tr} (P_s L_1 L_2 L_3)}{\text{Tr } P_s}. \quad (9)$$

We find

$$\begin{aligned} C_{QQQ}^1 &= \frac{1}{6} (27 \text{Tr } L_1 \text{Tr } L_2 \text{Tr } L_3 - 9 \text{Tr } L_1 \text{Tr} (L_2 L_3) \\ &\quad - 9 \text{Tr } L_2 \text{Tr} (L_1 L_3) - 9 \text{Tr } L_3 \text{Tr} (L_1 L_2) \\ &\quad + 3 \text{Tr} (L_1 L_2 L_3) + 3 \text{Tr} (L_1 L_3 L_2)) \end{aligned} \quad (10)$$

$$\begin{aligned} C_{QQQ}^8 &= \frac{1}{24} (27 \text{Tr } L_1 \text{Tr } L_2 \text{Tr } L_3 + 9 \text{Tr } L_1 \text{Tr} (L_2 L_3) \\ &\quad - 9 \text{Tr } L_3 \text{Tr} (L_1 L_2) - 3 \text{Tr} (L_1 L_3 L_2)) \end{aligned} \quad (11)$$

$$\begin{aligned} C_{QQQ}^{8'} &= \frac{1}{24} (27 \text{Tr } L_1 \text{Tr } L_2 \text{Tr } L_3 + 9 \text{Tr } L_3 \text{Tr} (L_1 L_2) \\ &\quad - 9 \text{Tr } L_1 \text{Tr} (L_2 L_3) - 3 \text{Tr} (L_1 L_2 L_3)) \end{aligned} \quad (12)$$

$$\begin{aligned} C_{QQQ}^{10} &= \frac{1}{60} (27 \text{Tr } L_1 \text{Tr } L_2 \text{Tr } L_3 + 9 \text{Tr } L_1 \text{Tr} (L_2 L_3) \\ &\quad + 9 \text{Tr } L_2 \text{Tr} (L_1 L_3) + 9 \text{Tr } L_3 \text{Tr} (L_1 L_2) \\ &\quad + 3 \text{Tr} (L_1 L_2 L_3) + 3 \text{Tr} (L_1 L_3 L_2)). \end{aligned} \quad (13)$$

Finally we obtain for the color averaged correlator of the three quark system, C_{QQQ}^{av} , the relation

$$\begin{aligned} C_{QQQ}^{\text{av}} &= \frac{1}{27} C_{QQQ}^1 + \frac{8}{27} C_{QQQ}^8 + \frac{8}{27} C_{QQQ}^{8'} + \frac{10}{27} C_{QQQ}^{10} \\ &= \frac{1}{27} \text{Tr } L_1 \text{Tr } L_2 \text{Tr } L_3. \end{aligned} \quad (14)$$

We note that the two octet correlators C_{QQQ}^8 and $C_{QQQ}^{8'}$ are the same when calculated on the lattice. The free energy of the symmetry state s can be obtained from the correlator in the usual way

$$F_{QQQ}^s(T) = -T \ln \langle C_{QQQ}^s(T) \rangle, \quad (15)$$

where $\langle \cdot \rangle$ stands for thermal averages taken after gauge fixing. We have suppressed the position dependence on both sides of (15).

In the following section we will discuss briefly the behavior of the free energies of the three quark system for small couplings and short distances.

III. F_{QQQ}^s AT SHORT DISTANCES

In the perturbative expansion of the free energy of QQQ -systems the contribution of the three gluon vertex vanishes for symmetry reasons [13]. Therefore, neglecting self energy contributions, to order g^4 the free energy

¹ For convenience we write L_i instead of $L(\mathbf{x}_i)$.

F_{QQQ}^s decomposes into the sum of three diquark free energies F_{QQ}^t , which can be in an anti-symmetric antitriplet ($t = \bar{3}$) or in a symmetric sextet ($t = 6$) state. The behavior of these diquark free energies at small distances to lowest order are Coulombic

$$F^t(R, T) = C_2(t) \frac{\alpha}{R}, \quad (16)$$

where $\alpha = \frac{g^2}{4\pi}$ and R is the separation of the static quarks in the QQ -system. The Casimir factor $C_2 = \text{Tr}(t_1^a t_2^a)$ depends on the color channel t the diquark system is in and can be found in table I. In order to obey the permutation relations given for the QQQ -system in (4) - (7), the QQQ -singlet state must be composed of QQ -anti-triplets, the QQQ -decuplet of QQ -sextets and the QQQ -octets are a mixture of QQ -anti-triplets and -sextets. Thus, we have for small distances

$$F_{QQQ}^1(\mathbf{R}, T) = \sum_{i < j} -\frac{2}{3} \frac{\alpha}{R_{ij}} + \tilde{k}_1(T) \quad (17)$$

$$F_{QQQ}^8(\mathbf{R}, T) = -\frac{2}{3} \frac{\alpha}{R_{12}} - \frac{1}{6} \frac{\alpha}{R_{13}} + \frac{1}{3} \frac{\alpha}{R_{23}} + \tilde{k}_8(T) \quad (18)$$

$$F_{QQQ}^{8'}(\mathbf{R}, T) = \frac{1}{3} \frac{\alpha}{R_{12}} + \frac{1}{6} \frac{\alpha}{R_{13}} - \frac{2}{3} \frac{\alpha}{R_{23}} - \tilde{k}_{8'}(T) \quad (19)$$

$$F_{QQQ}^{10}(\mathbf{R}, T) = \sum_{i < j} \frac{1}{3} \frac{\alpha}{R_{ij}} + \tilde{k}_{10}(T), \quad (20)$$

where R_{ij} denotes the distance between the i th and j th quark (see sec. IV B for details), $\mathbf{R} = (R_{12}, R_{13}, R_{23})$. The self energy contributions \tilde{k}_i with $i = 1, 8, 8', 10$ are temperature dependent and at small separations related to the free energy of a single static quark in the corresponding color state, $F_Q^{(s)}(T)$ (see sec. VII for details). Thus $\tilde{k}_1(T) = 0$, $\tilde{k}_8(T) = \tilde{k}_{8'}(T) = F_Q^{(8)}(T)$ and $\tilde{k}_{10}(T) = F_Q^{(10)}(T)$. As can be seen easily from (17) and (20), the singlet state of the QQQ -system is attractive, because the QQ -antitriplet is, and the decuplet state is repulsive, as the QQ -sextet is. Moreover, the QQQ -singlet free energy is temperature independent at small distances like the QQ -singlet free energy is [15]. For the octet channels the situation is more complicated due to the contribution of both anti-triplet and sextet free energies. We can, however, compute the lowest order behavior of the QQQ free energies for equilateral geometries for all color channels. Table I summarizes the Casimir factors for the free energies of the different color channels for all the quark systems $Q\bar{Q}$, QQ and QQQ . One recovers the lowest order behavior of the free energy in some symmetry state t (equilateral geometries for the QQQ -systems only) that depends on the separation of the static quarks by using (16), where R is now the separation of the static quarks in the $Q\bar{Q}$ - and QQ -systems

system	1	$\bar{3}$	6	8	10
$Q\bar{Q}$	-4/3			+1/6	
QQ		-2/3	+1/3		
QQQ^\dagger	-2			-1/2*	+1

TABLE I: Casimir factor for color symmetry state t , $C_2(t) = \text{Tr}(T_1^a T_2^a)$.

† equilateral geometries, * average of both octets.

and the edge length of the equilateral geometry in the QQQ case. See sec. IV B for details on the geometric configuration of the three static quarks. We see, that the average of both QQQ -octet free energies (which is accessible to lattice calculations) for equilateral geometries is expected to be weakly attractive.

At larger distances, the pairwise interactions of the static quarks should receive temperature dependent contributions and the Coulomb terms in (17) - (20) have to be replaced by the full diquark free energies $F_{QQ}^t(R, T)$ of the corresponding color channel t . In this case, (17) - (20) generalize to

$$F_{QQQ}^1(\mathbf{R}, T) = \sum_{i < j} F_{QQ}^{\bar{3}}(R_{ij}, T) + k_1(T) \quad (21)$$

$$F_{QQQ}^8(\mathbf{R}, T) = F_{QQ}^{\bar{3}}(R_{12}) + \frac{1}{4} F_{QQ}^{\bar{3}}(R_{13}) + F_{QQ}^6(R_{23}) + k_8(T) \quad (22)$$

$$F_{QQQ}^{8'}(\mathbf{R}, T) = F_{QQ}^6(R_{12}) - \frac{1}{4} F_{QQ}^{\bar{3}}(R_{13}) + F_{QQ}^{\bar{3}}(R_{23}) + k_{8'}(T) \quad (23)$$

$$F_{QQQ}^{10}(\mathbf{R}, T) = \sum_{i < j} F_{QQ}^6(R_{ij}, T) + k_{10}(T), \quad (24)$$

where the $k_i(T)$ with $i = 1, 8, 8', 10$ account for the self energy contributions not included in the diquark free energies. It was shown in [14] that the residual T -dependence of the QQ -anti-triplet free energy at small distances in the deconfined phase can be removed by subtracting the free energy of a single static quark $F_Q(T) \equiv \frac{1}{2} \lim_{R \rightarrow \infty} F_{QQ}^1(R, T)$. We therefore expect $k_1(T) = -3F_Q(T)$, which guarantees the cancelation of self energy contributions stemming from $F_{QQ}^{\bar{3}}$, leaving F_{QQQ}^1 temperature independent at small separations. Moreover, at large separations, the self energy contributions for the QQQ -system should be independent from the particular color channel the system is in, leading to $k_1(T) = k_8(T) = k_{8'}(T) = k_{10}(T) = -3F_Q(T)$. We will show in sections V, VI and VII that this reasoning is indeed correct for temperatures $T > T_c$. Indeed, we will show that the decomposition of interactions in 3-quark systems in terms of 2-quark interactions as suggested by

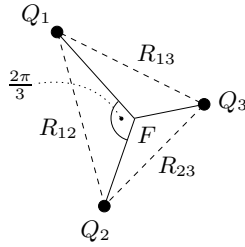


FIG. 1: Inter quark distances. F is the Fermat point of the triangle.

(21)-(24) holds for $T > T_c$.

We finally note, that the QQQ -octet free energy obtained from the lattice is the average of F_{QQQ}^8 and $F_{QQQ}^{8'}$, as will be shown in sec. IV. Consequently, we expect the lattice QQQ -octet free energy for equilateral geometries to obey

$$F_{QQQ}^8(R, T) = \frac{3}{2} \left(F_{QQQ}^8(R, T) + F_{QQQ}^6(R, T) \right) - 3F_Q(T), \quad (25)$$

where R is the edge length of the equilateral triangle.

IV. SIMULATION DETAILS

We will now present the details of our simulation.

A. Simulation

We used gauge field configurations generated on $32^3 \times 4$ and $32^3 \times 8$ lattices in pure gauge theory with the tree level-Symanzik improved gauge action at several couplings above and below the critical coupling [16, 17]. In 2-flavor staggered QCD we reexamined configurations on a $16^3 \times 4$ lattice for several different couplings at bare quark mass $m/T = 0.4$, where for fermions the p4-action and for the gauge fields again the tree level-Symanzik improved gauge action were used [18, 19, 20]. The scale was set using the string tension, σ , at $T = 0$ following [21] and use it to express all dimensionful observables. On all configurations we calculated the three point correlation functions of Polyakov loops (10) - (13), (14) in a manner explained below.

The operators in (10) - (13) are not manifestly gauge independent and therefore a gauge fixing procedure must be applied to our gauge configurations. We use Coulomb gauge for our calculations, in which the singlet free energies of the $Q\bar{Q}$ -system are related to a gauge independent definition in terms of dressed Polyakov lines [22]. Note that an operator dependence might still persist within this definition [23].

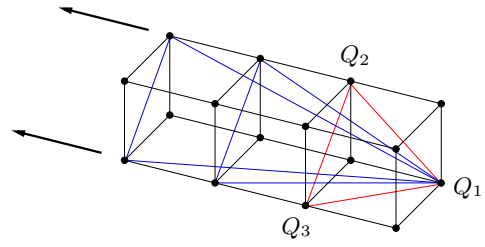


FIG. 2: Calculation of the three point correlation function of the Polyakov loop.

B. Calculation technique

We first fix the notation for the geometries of the three quark system. In fig. 1 we show three quarks Q_i forming a triangle and their distances R_{ij} , where $i, j = 1, 2, 3$. The perimeter of the triangle is then simply given by

$$P = \sum_{i < j} R_{ij}. \quad (26)$$

This is also the total length of a Δ -shaped string, i. e. a string connecting the three quarks along the edges of the triangle. Another possible string shape is a Y-shaped string, where the flux tube emanates from each of the three quarks and has a junction at the Fermat point F of the triangle. The total length of such a Y-shaped string is

$$L = \left[\frac{1}{2} \sum_{i < j} R_{ij}^2 + 2\sqrt{3}A_\Delta \right]^{\frac{1}{2}}, \quad (27)$$

where A_Δ is the area of the triangle [6]. The inner angles at the vertices of the triangle are assumed to be smaller than $\frac{2\pi}{3}$, which is the case for all triangles considered in this work. The angle between any two arms of the Y-shaped flux tube is always $\frac{2\pi}{3}$. For equilateral triangles we have the simple relation $P = \sqrt{3}L$. In this work we examine only isosceles triangles, where we set $R_{12} = R_{13} = R_s$ to be the equally long edges and $R_{23} = R_b$ to be the length of the base edge. For equilateral triangles we have $R_{ij} = R$ for all $i, j = 1, 2, 3$.

The three point correlation functions of the Polyakov loop are now obtained as follows (see fig. 2). At the positions of the Q_i , we calculate the correlation functions (10) - (13), (14) and compute the average of the correlation function for those Q_i with the same $\{R_{ij}\}$. We obtain a new set of $\{R_{ij}\}$ by holding Q_1 fixed, whereas the two other vertices of the triangle Q_2 and Q_3 are moved simultaneously one point of the lattice in one direction (here: to the left). The base edge R_b connecting these two points preserves thereby its length, which is $R_b/a = n\sqrt{2}$, where a denotes the lattice spacing and $1 \leq n < \frac{N_a}{2}$ is an integer and describes the number of elementary cells the procedure starts with. The two other edges have equal lengths $R_s/a = \sqrt{m^2 + n^2}$, where m is another integer

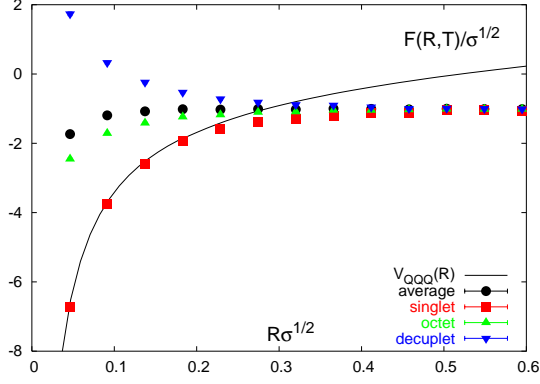


FIG. 3: Free energies in different color channels obtained on a $32^3 \times 8$ lattice at $T/T_c = 6$ from simulations in quenched QCD.

which runs between $n \leq m < \frac{N_c}{2}$ for every n . Therefore for every n we obtain one equilateral ($n = m$) and several isosceles ($n < m < \frac{N_c}{2}$) triangles. We start with $n = 1$ and repeat the procedure until $n = \frac{N_c}{2} - 1$. We apply this method in both directions of all three spatial dimensions before sweeping Q_1 over the entire spatial lattice. We will denote the configuration averages of the correlation functions (10) - (13) and (14) by C_{QQQ}^s with $s = 1, 8, 10$, av from now on.

C. Renormalization

We construct all correlation functions using renormalised thermal Wilson lines $L^{\text{ren}}(T)$, which are obtained from the bare ones calculated on lattices with temporal extent N_τ through multiplicative renormalisation,

$$L^{\text{ren}}(T) = (Z(g^2))^{N_\tau} L(g^2, N_\tau), \quad (28)$$

where $Z(g^2)$ is the multiplicative renormalisation constant determined in [15], g is the bare coupling and N_τ is the temporal extent of the lattice L is calculated on. The renormalization constants only depend on the bare coupling [24, 25] (and in addition on the bare quark masses in full QCD) and furthermore are equivalent at zero and finite temperature [26]. The renormalised three point correlation function of the thermal Wilson lines, $C^{\text{ren}}(T)$, is then obtained from the bare one, $C_{QQQ}(g^2, N_\tau)$, by

$$C_{QQQ}^{\text{ren}}(T) = (Z(g^2))^{3N_\tau} C_{QQQ}(g^2, N_\tau). \quad (29)$$

V. RESULTS IN PURE GAUGE

In this section we will analyze the behavior of three quark free energies in different color channels above T_c . We compare results with the perturbative expressions obtained in section III as well as with results obtained for

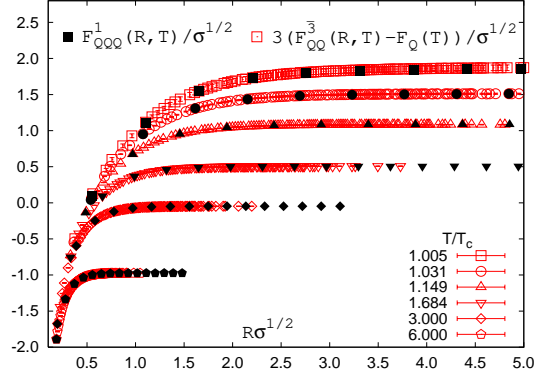


FIG. 4: $F_{QQQ}^1(R, T)$ and $3(F_{QQQ}^3(R, T) - F_Q(T))$ above T_c versus R , the edge length R of the equilateral triangles and QQ -distance, respectively.

QQ -systems in different color channels. Data for the QQ free energies have been taken from [14]. Below T_c we examine the string shape of the baryonic system and its structure in the different color channels.

A. Color Channels

In fig. 3 we show the free energies of three quark systems in different color channels and the average free energy for the QQQ -system for equilateral triangles of edge length R calculated on a $32^3 \times 8$ lattice at $T/T_c = 6$. One can see clearly, that the singlet is strongly, the octet weaker attractive and the decuplet repulsive in agreement with the perturbative findings presented in sec. III. For large R at a given temperature, all free energies in the different color channels approach a common value, i. e. the three quarks are screened independently of their color orientation. The singlet free energy becomes temperature independent at small distances and coincides with the baryonic $T = 0$ potential, $V_{QQQ}(R)$, (see also fig. 4), which is related to the quark-antiquark potential at vanishing temperature by the ratio of the different Casimir operators, i. e. $V_{QQQ}(R) = \frac{3}{2}V_{Q\bar{Q}}(R)$ for $R\Lambda_{QCD} \ll 1$. We obtain similar results for all other temperatures above T_c . We will discuss the screening of octet and decuplet free energies at small distances in sec. VII.

B. Free energies of equilateral geometries above T_c

We now compare the free energies of the QQQ -system with the free energy of the QQ -system above T_c . In fig. 4 we show $F_{QQQ}^1(R, T)$ and $3F_{QQQ}^3(R, T) - 3F_Q(T)$ versus the edge length R of the equilateral triangles and the QQ distance, respectively. According to (21) the second term is expected to be equal to the QQQ -singlet free energy at least at small distances, where genuine three body forces

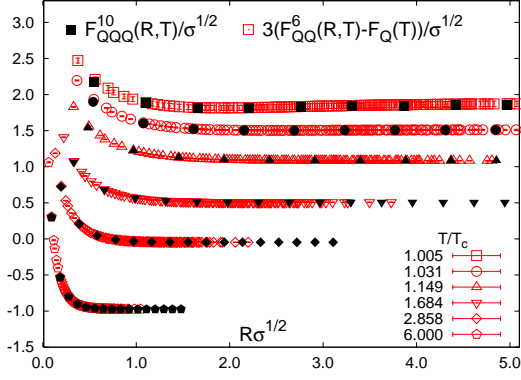


FIG. 5: $F_{QQQ}^{10}(R, T)$ and $3(F_{QQ}^6(R, T) - F_Q(T))$ above T_c versus R , the edge length R of the equilateral triangles and QQ -distance, respectively.

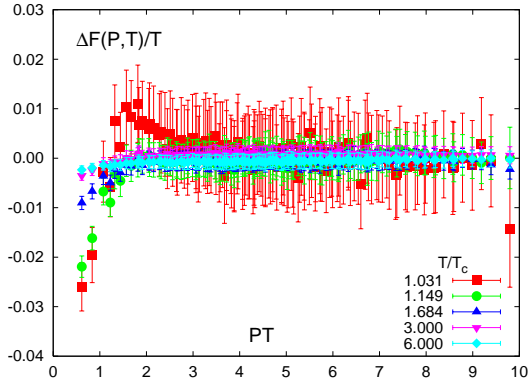


FIG. 6: $\Delta F(P, T) = F_{QQQ}^1(P, T) - \sum_i F_{QQ}^3(R_{ij}, T) + 3F_Q(T)$ above T_c versus the perimeter P for all geometries calculated.

are negligible. For all temperatures above T_c we indeed see that $F_{QQQ}^1(R, T)$ and $3F_{QQ}^3(R, T) - 3F_Q(T)$ coincide throughout the entire distance interval. In fig. 5 we show analogously $F_{QQQ}^{10}(R, T)$ and $3F_{QQ}^6(R, T) - 3F_Q(T)$. Again we observe that both observables do coincide. We obtain similar plots for $F_{QQQ}^8(R, T)$ in accordance with (25).

C. Free energies of isosceles geometries above T_c

In order to test whether the simple relation between free energies of a 3 quark system and the free energies of a 2 quark system plus self energy terms also holds for other geometries and temperatures above T_c , we calculate the difference $\Delta F(P, T) = F_{QQQ}^1(P, T) - \sum_{i<j} F_{QQ}^3(R_{ij}, T) + 3F_Q$. This is shown in fig. 6. If (21) also holds for these geometries, then $\Delta F(P, T)$ should vanish, which is fulfilled to a very good degree for all perimeters except the smallest ones. Again the same holds true also for the QQQ -decuplet free energy as is evident from fig. 7. This is possibly due to the effect, that the self energy of the

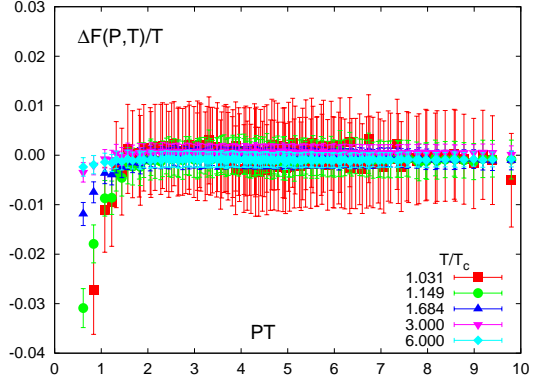


FIG. 7: $\Delta F(P, T) = F_{QQQ}^{10}(P, T) - \sum_{i<j} F_{QQ}^6(R_{ij}, T) + 3F_Q(T)$ above T_c versus the perimeter P for all geometries calculated.

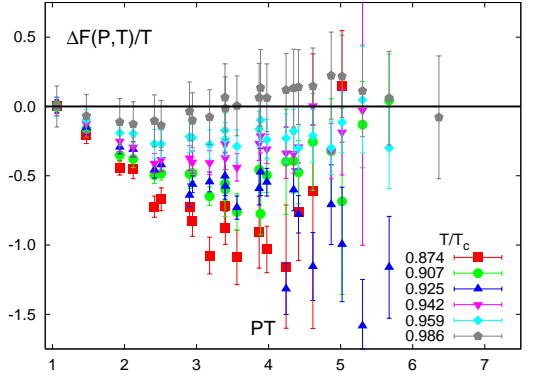


FIG. 8: $\Delta F(P, T) = F_{QQQ}^1(P, T) - \sum_{i<j} F_{QQ}^3(R_{ij}, T)$ below T_c versus the perimeter P for all geometries calculated. $\Delta F(P_{\min}, T)$ has been set to zero, where P_{\min} is the smallest perimeter calculated.

system is no longer the sum of the self energy of the individual static quarks at short distances but rather that of a single static quark in the corresponding color representation (see sec. VII).

Having now established that (21) and (24) hold for all isosceles geometries above T_c calculated in this work, it is clear that the screening length of the three quark system in the singlet state is the same as that of the antitriplet diquark state, which itself has been shown to be equal to that of the $Q\bar{Q}$ singlet state [14], therefore reflecting the properties of the thermal medium rather than that of a particular hadronic system.

Furthermore, we can apply the relations used in [14] to calculate entropy and internal energy from free energies of a QQ system also for the QQQ system. The entropy in the color singlet channel is defined by

$$S_{QQQ}^1(P, T) = \frac{\partial F_{QQQ}^1(P, T)}{\partial T} \quad (30)$$

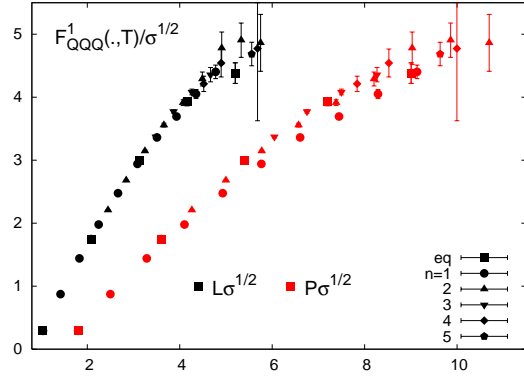


FIG. 9: $F_{QQQ}^1(., T)$ at $T/T_c = 0.925$ versus the Y-string length L and the perimeter P for equilateral geometries (eq) and geometries with base length $R_b\sqrt{\sigma} = n\sqrt{\sigma}\sqrt{2}$, where n is given in the legend.

and the internal energy in this channel is

$$U_{QQQ}^1(P, T) = -T^2 \frac{\partial F_{QQQ}^1(P, T)/T}{\partial T}. \quad (31)$$

We then obtain for the entropy

$$\lim_{P \rightarrow 0} S_{QQQ}^1(P, T) = 0, \quad (32)$$

i. e. the entropy contribution in the free energy of the QQQ singlet color channel vanishes at small distances. Moreover, we find for the internal energy, that

$$\lim_{P \rightarrow 0} U_{QQQ}^1(P, T) = \lim_{P \rightarrow 0} V_{QQQ}(P), \quad (33)$$

where $V_{QQQ}(P) = \frac{1}{2} \sum_{i < j} V_{Q\bar{Q}}(R_{ij})$ and $V_{Q\bar{Q}}(r)$ is the quark-anti-quark potential at $T = 0$. This means that the internal energy becomes T -independent for small perimeters and thus, together with (30), the singlet free energy itself is T -independent for small perimeters, as was already seen in sec. V A. This behavior is already known for $Q\bar{Q}$ singlet free energies and reflects the fact that the baryonic system is less and less effected by the surrounding thermal medium when going to smaller and smaller perimeters.

D. Free energies below T_c

We now examine the QQQ free energies below T_c . We start by looking at the relation between the QQQ -singlet and the QQ -antitriplet free energies. If F_{QQQ}^1 can be expressed in terms of the sum of $F_{QQ}^3(R_{ij}, T)$ also below T_c , i. e. if a Δ -ansatz for the flux tube shape together with the same string tension holds, then F_{QQQ}^1 is a function of the perimeter only and $\Delta F(P, T) = F_{QQQ}^1(P, T) - \sum_{i < j} F_{QQ}^3(R_{ij}, T)$ should be equal to a T -dependent constant $k(T)$ for all P . In fig. 8 we show

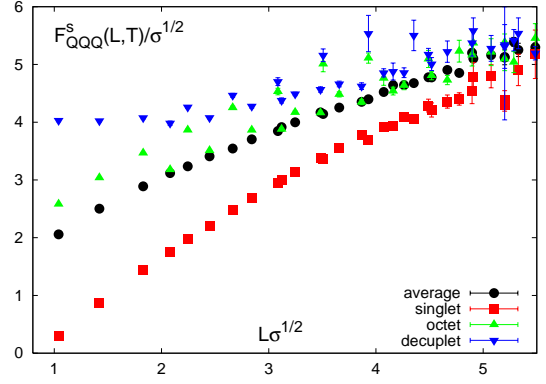


FIG. 10: Free energies of the color channels versus the Y-string length L at $T/T_c = 0.925$ for all geometries calculated.

$\Delta F(P, T)/T$ for $T < T_c$ versus the perimeter, P , for different geometries. Here we have set $\Delta F(P_{\min}, T) = 0$, where P_{\min} is the smallest perimeter calculated. We can see clear deviations of $\Delta F(P, T)$ to smaller values, most strongly for the lowest temperatures, deviations from zero becoming smaller with growing temperature. For $T/T_c = 0.986$ we have $\Delta F(P, T) \approx 0$. Hence, $F_{QQQ}^1(P, T)$ can not be expressed in terms of the sum of $F_{QQ}^3(R_{ij}, T)$ except close to the critical temperature. We are left with two possibilities now. First, we could still have a Δ -shaped flux tube, but with a different string tension than that observed for the QQ -antitriplet. Since we see $\Delta F(P, T) < 0$, we would expect the string tension to be smaller than in the QQ -antitriplet. In this case the perimeter P would still be the right distance measure for the QQQ -singlet free energy, i. e. F_{QQQ}^1 should be a smooth function of P for all geometries. Or, secondly, the flux tube is Y-shaped and L is the right distance measure. In this case, F_{QQQ}^1 should be a smooth function of L for all geometries in which a flux tube can form.

To elaborate more on the shape of the flux tube, we take a closer look at the QQQ -singlet free energy at a particular temperature below T_c . We analyze the free energy for different geometries as a function of L and P . For equilateral triangles a simple geometrical relation exists between the length of a Y-shaped flux tube L and the length of a Δ -shaped flux tube P , which is $P = \sqrt{3}L$. Hence for equilateral geometries the QQQ -singlet free energy is a smooth function in both Ansätze. For more general geometries like the isoscele triangles we calculated, no simple relation between L and P exists. This may help to clarify the situation more directly. Therefore we plot the QQQ -singlet free energy at $T/T_c = 0.925$ versus the Y-string length L and the perimeter P . This is shown in fig. 9 for equilateral geometries and also for isoscele geometries up to $n = 5$ (see sec. IV B). We observe that the QQQ -singlet free energy is indeed a smooth function of L for all geometries calculated. On the other hand, when the free energy is plotted versus the perimeter P different branches become visible depending on the geometry.

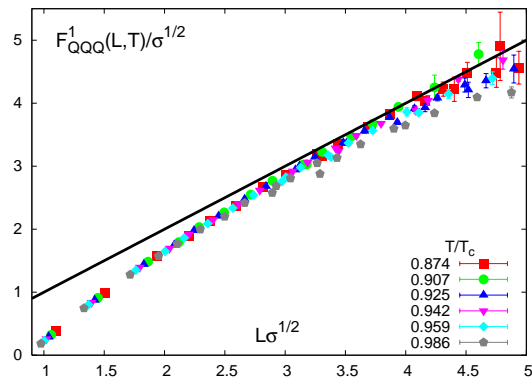


FIG. 11: $F^1_{QQQ}(L, T)$ below T_c versus the Y-string length L for all geometries.

This is most prominent for the $n = 1$ triangles. Therefore we find strong hints, that the shape of the flux tube in the QQQ -singlet system is indeed that of the Y-ansatz and its string length L is the right distance measure for the system.

Having established this, we take a look at the other color channels below T_c and analyze whether they display a smooth behavior as function of L as well. In fig. 10 we show the different color channels of the QQQ -free energy at $T/T_c = 0.925$ over the Y-string length L . We see again that the singlet is the most attractive channel followed by the average free energy, which is also a smooth function of L . The octet channel is still attractive, but weaker so than the average free energy. The decuplet free energy is attractive for large L but becomes flat at smaller L , possibly hinting at a turnover and at a repulsive behavior at even smaller L . Both the decuplet and the octet channel are not smooth functions over either distances L and P , but become volatile for $L\sqrt{\sigma} \gtrsim 2$. This suggests that no flux tube forms in these two channels, besides that the octet free energy shows an overall attractive behavior.

Finally, we examine more closely the temperature dependence of F^1_{QQQ} . In fig. 11 we show the renormalised QQQ -singlet free energy versus L for all temperatures below T_c . We observe $F^1_{QQQ}(L, T)$ to nearly coincide at distances $L\sqrt{\sigma} \lesssim 4$ for all temperatures $T/T_c \leq 0.959$. We see that at large distances the free energies approach $F(L, T) = \sigma L$ represented by the black line in fig. 11, where σ denotes the string tension in a $Q\bar{Q}$ -system. The phenomenon of an almost T -independent string tension has also been observed in [7], using a fit ansatz in full QCD. As was already seen in fig. 8, at $T/T_c = 0.986$ we observe deviations to smaller values. This might be due to flux tube broadening setting in near T_c , leading to an overlapping of the three branches of the Y-shaped flux tube. Filling the space between the three static quarks the separation dependence of the singlet free energy is effectively described by the Δ -Ansatz at these temperatures.

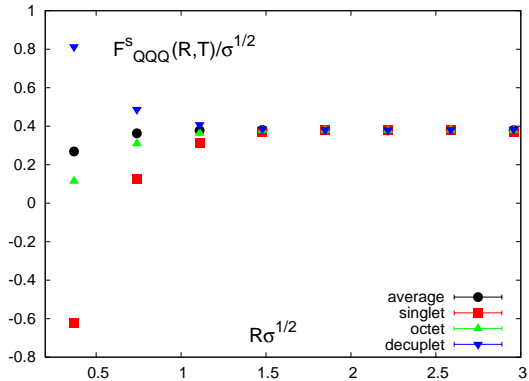


FIG. 12: Free energies in different color channels in 2-flavor QCD from calculations on a $16^3 \times 4$ lattice at $T/T_c = 1.99$.

VI. RESULTS IN 2-FLAVOR QCD

In this section we analyse the QQQ -free energies obtained on a $16^3 \times 4$ lattice in 2-flavor QCD with a bare quark mass of $\frac{m}{T} = 0.4$. For further details, see sec. IV. Data for the QQ free energies is again taken from [14].

A. Color Channels

In fig. 12 we show the free energies of three quark systems with equilateral geometries in different color channels at $T/T_c = 1.99$. Like in the pure gauge case, we observe the singlet to be strongly, the octet weaker attractive and the decuplet to be repulsive. For large distances R the free energies in all color channels approach a common value. Again, we obtain similar results for all $T > T_c$.

B. Singlet free energy

We now compare the free energy of the QQQ -singlet with the free energy of the QQ -antitriplet for 2-flavor QCD. In fig. 13 we show $F^1_{QQQ}(R, T)$ and $3F^{\bar{3}}_{QQ}(R, T) - 3F_Q(T)$ versus the edge length R of the equilateral triangles and QQ distance, respectively. As in pure gauge theory, both curves coincide for all temperatures above T_c . Thus we find the QQQ -singlet free energy of equilateral geometries can be described as the sum of three QQ -antitriplet free energies plus self energy terms as well in 2-flavor QCD above T_c .

Below T_c we expect to see string breaking also in the QQQ -singlet free energy, the breaking mechanism being more involved than in the $Q\bar{Q}$ case [7]. Indeed, except at $T/T_c = 0.97$, where both quantities agree, we see deviations for the QQQ -singlet from the simple relation to the QQ free energies. In fig. 14 we compare $F^1_{QQQ}(L, T)$ in 2-flavor QCD ($T/T_c = 0.88, 0.91$) and pure gauge theory ($T/T_c = 0.874, 0.907$) for all geometries calculated.

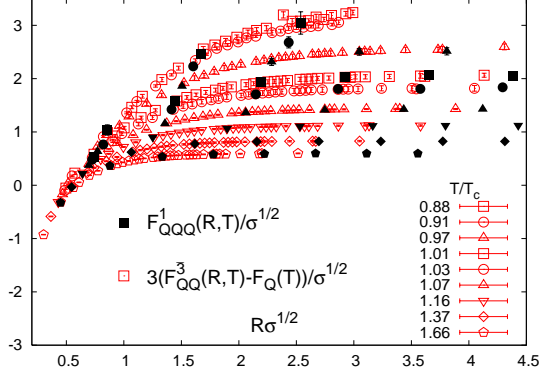


FIG. 13: $F_{QQQ}^1(R, T)$ and $3(F_{QQ}^3(R, T) - F_Q(T))$ versus R , the edge length of the equilateral triangles and QQ -distance, respectively.

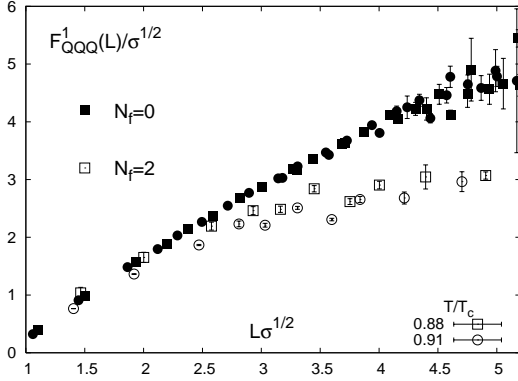


FIG. 14: Comparison of $F_{QQQ}^1(L, T)$ in 2-flavor QCD (open symbols) and SU(3) pure gauge theory (filled symbols) for two temperatures below T_c .

Here the pure gauge data have been obtained from simulations on a $32^3 \times 4$ lattice. The $N_f = 2$ free energies start to deviate from the pure gauge result already at short distances to smaller values and eventually become flat. Specifying a definite value for the string breaking distance is quite difficult given the present data. Nevertheless we can give a rough estimate for the distance at which the pure gauge free energies assumes the asymptotic value of the 2-flavor free energies, which is $L\sqrt{\sigma} \approx 3$. For higher T , this distance becomes smaller. The string breaking distance for the $Q\bar{Q}$ singlet free energies has been determined in [24] as the distance where the $T = 0$ potential assumes the large distance asymptotic value of the free energy. This lead to values between $2.8/\sqrt{\sigma}$ for $T/T_c = 0.874$ and $1.7/\sqrt{\sigma}$ close to T_c .

C. Decuplet free energies

For the QQQ -decuplet free energies we show $F_{QQQ}^{10}(R, T)$ and $3(F_{QQ}^6(R, T) - F_Q(T))$ for equilateral

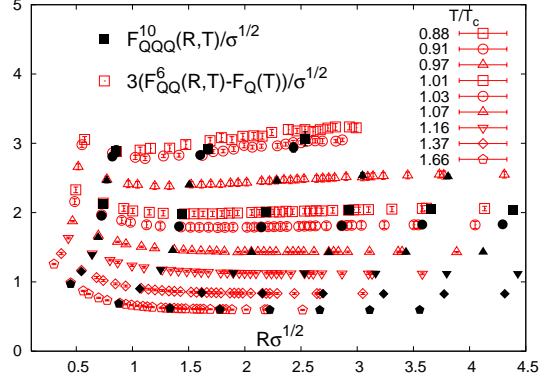


FIG. 15: $F_{QQQ}^{10}(R, T)$ and $3(F_{QQ}^6(R, T) - F_Q(T))$ versus R , the edge length of the equilateral triangles and QQ -distance, respectively.

geometries in fig. 15. Like in pure gauge theory, we observe both quantities to coincide for all temperatures above T_c and distances R . The situation below T_c is analogous to the singlet case. At the temperature closest to T_c both quantities coincide for all R , at smaller T we observe deviations to smaller values for $F_{QQQ}^{10}(R, T)$.

Hence we see, that the singlet (decuplet) QQQ free energy can be described as a sum of antitriplet (sextet) QQ free energies and the self energy contributions of the three quarks above T_c (Eqs (21) and (24)) also in 2-flavor QCD. Again, we obtain similar plots for $F_{QQQ}^8(R, T)$ in accordance with (25).

VII. SCREENING OF OCTET AND DECUPLET FREE ENERGIES

As was shown in [14], the screening of diquark free energies in the anti-triplet and sextet representation at small distances becomes identical to the screening of a single fermion in a color anti-triplet and sextet representation, respectively. This holds for all temperatures in 2-flavor QCD and in the deconfinement phase of SU(3) pure gauge theory.

We will now show, that analogous statements are true in the deconfinement phase for octet free energies of the $Q\bar{Q}$ -system and for octet and decuplet free energies of the QQQ -system, as we have proposed in sec. III.

When combining singlet and octet free energies or singlet and decuplet free energies in proportion to the corresponding Casimir factors (cf. Tab. I) such that the repulsive and attractive Coulombic contributions cancel, we

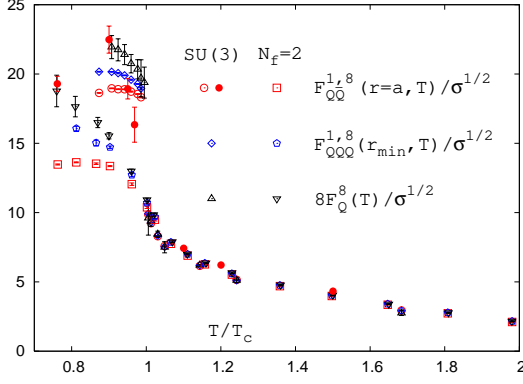


FIG. 16: Comparison of singlet and octet free energies at small distances with the free energy of a static fermion in the adjoint representation. We have used $F_{Q\bar{Q}}^{1,8}(R=a, T) = F_{Q\bar{Q}}^1(R=a, T) + 8F_{Q\bar{Q}}^8(R=a, T)$ and $F_{Q\bar{Q}}^{1,8}(R_{\min}, T) = -2F_{Q\bar{Q}}^1(R_{\min}, T) + 8F_{Q\bar{Q}}^8(R_{\min}, T)$. This particular combination of $Q\bar{Q}$ - and QQQ -free energies shown eliminates the short distance Coulomb terms contributing to them according to (34) - (36). Open symbols: $N_\tau = 4$ data, closed symbols: $N_\tau = 8$ data. For the QQQ -free energies we used equilateral geometries with edge length $R_{\min} = \sqrt{2}a$.

expect to find

$$\lim_{R \rightarrow 0} \left(F_{Q\bar{Q}}^{(1)}(R, T) + 8F_{Q\bar{Q}}^{(8)}(R, T) \right) \quad (34)$$

$$= \lim_{r \rightarrow 0} \left(-2F_{QQQ}^{(1)}(R, T) + 8F_{QQQ}^{(8)}(R, T) \right) \quad (35)$$

$$= 8F_Q^{(8)}(T) \quad (36)$$

and

$$\lim_{R \rightarrow 0} \left(F_{QQQ}^{(1)}(R, T) + 2F_{QQQ}^{(10)}(R, T) \right) = 2F_Q^{(10)}(T) \quad (37)$$

where R stands for the edge length of the equilateral geometries in the case of QQQ free energies; $F_Q^{(8)}(T)$ and $F_Q^{(10)}(T)$ are the free energies of a static quark in a color octet and decuplet representation, respectively. The latter are given by the corresponding Polyakov loop expectation values,

$$e^{-F_Q^{(D)}/T} = \langle L_D(\mathbf{x}) \rangle, \quad (38)$$

where $D = 8, 10$ and

$$L_8(\mathbf{x}) = \frac{1}{8} (9|L(\mathbf{x})|^2 - 1) \quad (39)$$

$$L_{10}(\mathbf{x}) = \frac{1}{10} (27L(\mathbf{x})^3 - 18|L(\mathbf{x})|^2 + 1) \quad (40)$$

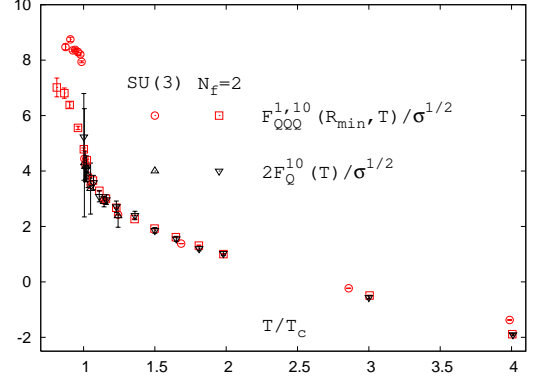


FIG. 17: Comparison of singlet and decuplet free energies at small distances with the free energy of a static fermion in the decuplet representation. We have used $F_{QQQ}^{1,10}(R_{\min}, T) = F_{QQQ}^1(R_{\min}, T) + 2F_{QQQ}^{10}(R_{\min}, T)$. This particular combination of QQQ -free energies shown eliminates the short distance Coulomb terms contributing to them according to (37). For the QQQ -free energies we used $N_\tau = 4$ data and again equilateral geometries with edge length $R_{\min} = \sqrt{2}a$.

are obtained through group theoretical relations. The Polyakov loops $\langle L_8 \rangle$ and $\langle L_{10} \rangle$ have been computed in [27]. We note here, that these quantities – unlike the Polyakov loop in the fundamental representation – do not have to vanish in the confinement phase of SU(3) pure gauge theory due to their vanishing triality.

(34) - (37) are indeed fulfilled for all temperatures above T_c as can be seen from Figs. 16 and 17. In particular, the combinations of singlet and octet free energies of the $Q\bar{Q}$ - and the QQQ -system coincide in the deconfinement phase (35), thus showing the screening at small distances to depend only on the color representation and not on the particular static quark system under consideration. Below T_c deviations become apparent in Fig. 16. The reason probably is, that the minimal distances used in the present analysis ($R = a$ for the $Q\bar{Q}$ -system and $R_{\min} = \sqrt{2}a$ for the QQQ -system respectively) are still too large at small temperatures to be a good approximation for the small distance limit in (34) - (37). In fact, the $N_\tau = 8$ data, where the lattice spacing a is only half as large at the same value of the temperature, agree much better at least close to T_c .

VIII. CONCLUSIONS

We have calculated the free energy of static three quark systems in different color channels in the quenched approximation and in 2-flavor QCD at finite temperature. We have shown that above the critical temperature the singlet and decuplet free energies of the three quark system can be described by the sum of the free energies of the corresponding diquark system plus self energy contributions. Therefore the screening of the singlet QQQ free energies is comparable to that of the $Q\bar{Q}$ free en-

ergies reflecting the screening properties of the thermal medium. Below T_c we found evidence for a Y-shaped flux tube in the quenched approximation for the singlet and color average channel. The string tension agrees with that deduced from $Q\bar{Q}$ -systems at $T = 0$ and has been found to be independent of temperature for $T/T_c \lesssim 0.959$ in the singlet color channel. In 2-flavor QCD we observed string breaking in the QQQ singlet free energies at distances around $3/\sqrt{\sigma}$. Moreover, we were able to show that at short distances the screening properties of octet free energies of the $Q\bar{Q}$ - and the QQQ -system and the decuplet free energies of the QQQ -system coincide with

those of a single static quark in the corresponding color state above T_c .

Acknowledgment

This manuscript has been authored under Contract No. DE-AC02-98CH10886 with the U. S. Department of Energy. O.V. and at an early stage K.H. have been supported by the Deutsche Forschungsgemeinschaft (DFG) under grant GRK 881.

-
- [1] R. Sommer and J. Wosiek, Nucl. Phys. B **267**, 531 (1986)
 - [2] G. S. Bali, Phys. Rept. **343**, 1 (2001)
 - [3] C. Alexandrou, P. De Forcrand and A. Tsapalis, Phys. Rev. D **65**, 054503 (2002)
 - [4] T. T. Takahashi, H. Suganuma, Y. Nemoto and H. Matsufuru, Phys. Rev. D **65**, 114509 (2002)
 - [5] T. T. Takahashi and H. Suganuma, Phys. Rev. D **70**, 074506 (2004)
 - [6] V. G. Bornyakov *et al.* [DIK Collaboration], Phys. Rev. D **70** (2004) 054506
 - [7] V. G. Bornyakov *et al.*, Prog. Theor. Phys. **112**, 307 (2004)
 - [8] Ph. de Forcrand and O. Jahn, Nucl. Phys. A **755**, 475 (2005)
 - [9] D. S. Kuzmenko and Y. A. Simonov, Phys. Lett. B **494**, 81 (2000)
 - [10] J. Liao and E. V. Shuryak, Nucl. Phys. A **775**, 224 (2006)
 - [11] S. Nadkarni, Phys. Rev. D **34**, 3904 (1986)
 - [12] S. Nadkarni, Phys. Rev. D **33**, 3738 (1986)
 - [13] J. M. Cornwall, Phys. Rev. D **54**, 6527 (1996)
 - [14] M. Döring, K. Hübner, O. Kaczmarek and F. Karsch, Phys. Rev. D **75**, 054504 (2007)
 - [15] O. Kaczmarek, F. Karsch, P. Petreczky and F. Zantow, Phys. Lett. B **543**, 41 (2002)
 - [16] P. Weisz, Nucl. Phys. B **212**, 1 (1983)
 - [17] P. Weisz and R. Wohlert, Nucl. Phys. B **236**, 397 (1984)
 - [18] F. Karsch, E. Laermann and A. Peikert, Nucl. Phys. B **605**, 579 (2001)
 - [19] C. R. Allton *et al.*, Phys. Rev. D **66**, 074507 (2002)
 - [20] C. R. Allton *et al.*, Phys. Rev. D **68**, 014507 (2003)
 - [21] B. Beinlich, F. Karsch and A. Peikert, Phys. Lett. B **390**, 41 (1997)
 - [22] O. Philipsen, Phys. Lett. B **535**, 138 (2002)
 - [23] O. Jahn and O. Philipsen, Phys. Rev. D **70**, 074504 (2004)
 - [24] O. Kaczmarek and F. Zantow, Eur. Phys. J. C **43**, 63 (2005)
 - [25] O. Kaczmarek, S. Gupta and K. Hübner, PoS(LATTICE 2007)195 arXiv:0710.2277 [hep-lat].
 - [26] O. Kaczmarek, PoS C **POD07**, 043 (2007)
 - [27] S. Gupta, K. Hübner and O. Kaczmarek, in preparation